POAC'15
Trondheim, Norway

Proceedings of the 23rd International Conference on
Port and Ocean Engineering under Arctic Conditions
June 14-18, 2015
Trondheim, Norway

CHARACTERISTICS OF SEA CURRENTS IN NAVIGATIONAL STRAIT AKSELSUNDET IN SPITSBERGEN

A. Marchenko[1,2], Z. Kowalik[3], D. Brazhnikov[3], N. Marchenko[1], E. Morozov[4]
[1]Arctic Technology Department, UNIS, N-9171 Longyearbyen, Norway
[2]Department of Civil and Transport Engineering, NTNU, N-7491 Trondheim, Norway
[3]Institute of Marine Science, UAF, AK 99775-7220 Fairbanks, USA
[4]P.P.Shirshov Institute of Oceanology, RAS, 117997 Moscow, Russia

ABSTRACT
The study of tide induced jet flow in navigation strait Akselsundet in Spitsbergen is performed.Tidal measurements performed near the inner and outer shorelines of Akseløya Island crossing the entrance to the Van Mijen Fjord near the Akselsundet Strait showed a shift of the tidal phase over the island of 30 min. The measurements of surface currents performed with GPS drifters showed that the maximal current speed in the strait is close to 2.5m/s. Numerical simulations performed with an original model of tides in the fjords of the West Spitsbergen confirmed a phase shift of 30 min and high speeds of the sea current in the strait. A simplified box model of tides in the fjord was developed for the estimates of navigable window for the strait. Numerical estimates showed that mean duration of navigable window when the water speed in the strait is lower than 0.5 m/s is about 15 min, while the actual size of the window is varying from neap to spring tide.

INTRODUCTION

The Aselsundet Strait is located between Bellsund Bay and the Van Mijen Fjord of the West Spitsbergen. Bellsund Bay is the offshore part of the Van Mijen Fjord west of Akseløya Island. Coal boats up to 70.000 tons deadweight pass the strait on the way to and from the Kapp Amsterdam coal quay near coal mining settlement Svea in the end of the Van Mijen Fjord (Fig. 1). Navigational activity of coal boats in the Van Mijen Fjord is performed only in ice free season 5 months long from the end of June to November. During this time the coal produced over the winter and summer in Svea mines is expected to be transported from the coal quay. One passage of a coal boat through the Akselsundet strait occurs in three-five days.

The Norwegian pilot (2014) characterizes navigational conditions in the strait by tidal streams with eddies and speeds up to 5-6 knots (2.5-3 m/s). Coal boats pass the strait with assistance of tugboats in navigable window when the current speed is low. It happens two times per one period of semidiurnal tide 12.42 h. Navigable window is determined by the measurements of sea current speed from tugboats. The main goal of this paper is to estimate the navigable window and describe characteristics of tides around Akseløya Island.

Effect of jet flow formation in the constriction at the entrance to the fjord was described by Stigebrandt (1980). Local conditions in the strait between Svea Bay and Vallunden lake in the Van Mijen Fjord were investigated by Marchenko and Morozov (2013). In this paper we discover similar phenomena in the Akselsundet Strait at the entrance to the Van Mijen Fjord.

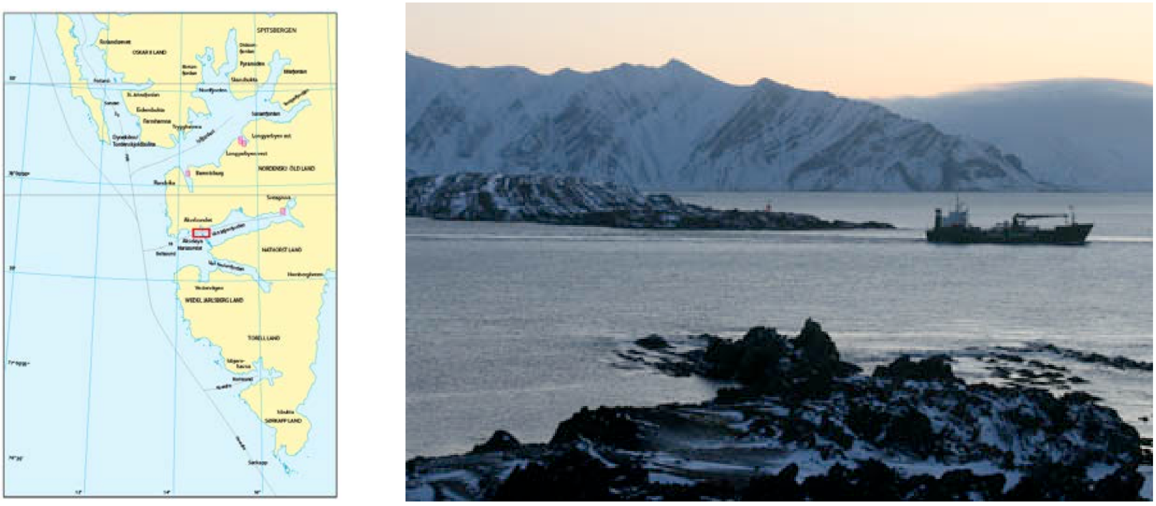

a) b)

Figure 1.Location of the Akselsundet Strait in Spitsbergen (a), a coal boat in the strait (b).

SEABED TOPOGRAPHY IN THE AKSELSUNDET STRAIT

A 3D view of seabed topography around Akseløya Island is shown in Fig. 2a. Coordinate axes x and y are directed to the east and north. The width of the Akselsundet Strait between the northern tip of Akseløya Island and the northern shore of the Van Mijen Fjord is about 1 km at the water level. Further to the east the strait extends so that the angle between Akseløya Island and the coastal slope of the Van Mijen Fjord is about 53^o (Fig. 2b). A 3D bathymetry near the entrance to the Van Mijen Fjord is shown in Fig. 3a, where plane z=0 shows the water-level. Vertical cross-sections of the strait bathymetry constructed by x=-3000 m and x=-2000 m are shown in Fig. 3b by blue and purple lines respectively. The deepest part of the Akselsundet Strait is associated with a channel bounded by vertical cross-sections S0 and S1 shown in Fig. 3b. The mean water depth in these cross-sections reaches 40 and 60 m respectively. The width of the channel is estimated as 300 m and 1000 m in the cross-sections S0 and S1 respectively.

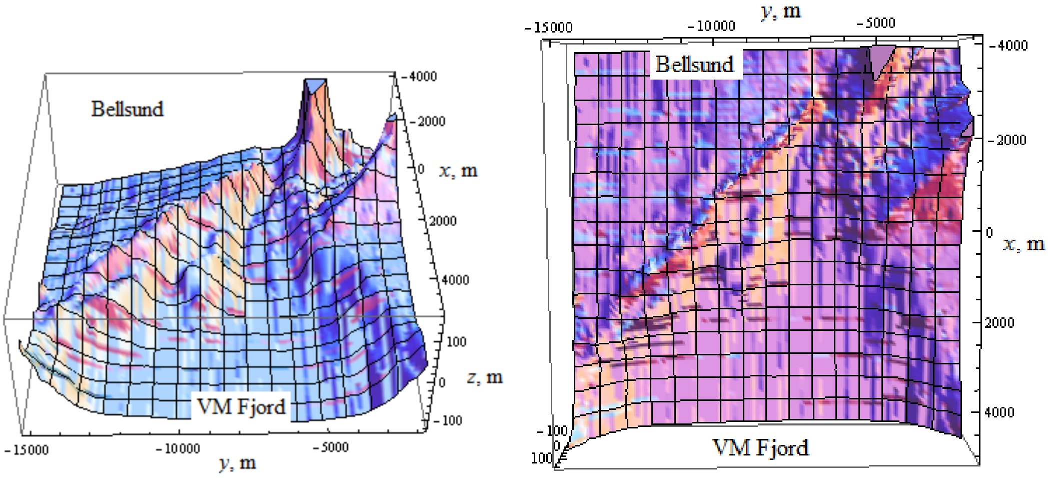

a) b)

Figure 2. Bathymetry around Akseløya Island: 3D view (a) and view from the top.

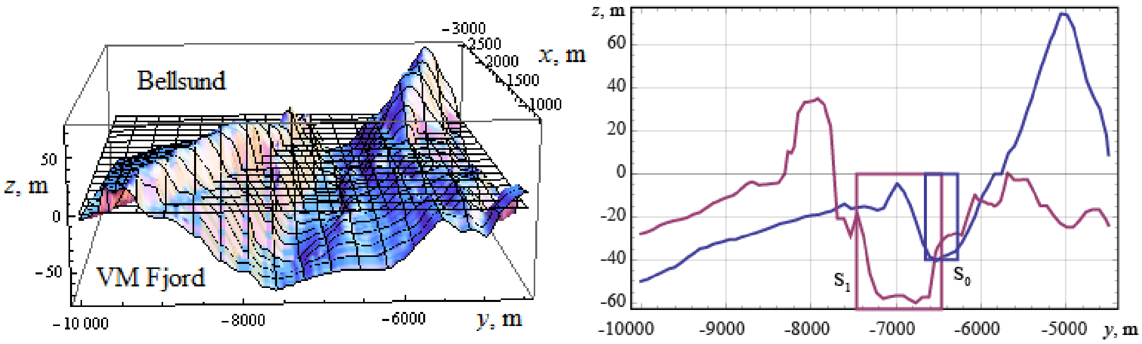

a) b)

Figure 3. 3D bathymetry of the Akselsundet Strait (a). Vertical cross-sections of the Akselsundet Strait are shown at x=-3000 m (blue line) and x=-2000 m (purple line) (b).

FIELD WORKS

Field works around Akseløya Island performed in 2010-2013 are specified in Table 1. The main goals of the field works were to measure tide induced variations of the water level near Bellsund and Van Mijen shores of Akseløya Island and in the Akselsundet Strait, and to measure the velocity of sea currents in the Akselsundet Strait. It is assumed that the tidal current in the strait is driven by the local gradient of the water pressure determined by the water level gradient in the strait. Synchronous measurements of the water pressure from different sides of Akseløya Island and sea current velocity in the strait can be used for the calculation of the transfer function showing the dependence of the sea current velocity in the strait from the water level gradient over Akseløya Island measured in two specific points.

Table 1. Field measurements performed near Akseløya Island.

Time	Water level measurements	Water velocity measurements
May 5-6, 2010	Deployment of temperature and pressure recorder SBE-39 on sea bottom near Bellsund and Van Mijen shores of Akseløya Island (red dots in Fig. 2a)	
August 30-31, 2011	Deployment of CTD SBE-37 on sea bottom near Akseløya Island (blue dot in Fig. 2a), pressure records by ADCP Aquadopp (green dot in Fig.2a)	Deployment of ADCP Aquadopp in the Akselsundet Strait (green dot in Fig.2a)
September 24-October 24, 2013	Deployment of temperature and pressure recorder SBE-39 on sea bottom near Bellsund and Van Mijen shores of Akseloya Island (red dots in Fig. 2a)	Deployment of surface drifters equipped with GPS antennas AstroDog-320 in the Akselsundet Strait

Field works were organized by the RV “Lance” in 2010 and by RV “Viking Explorer” in 2011 and 2013. In May 2010 the Van Mijen Fjord was covered by sea ice. The RV “Lance” was moored to the ice and the pressure sensors were delivered from the ship to Alseloya Island by snow scooters. Records of the water pressure at the sea bottom were performed using the SBE-39 and SBE-37 instruments placed at the bottom near the shoreline of Akseløya Island. In 2010 one of the SBE-39 sensors deployed near Van Mijen shore of the island was mounted on a rope fixed on the ice, while the other sensor deployed near the Bellsund shore of the island was fixed by a rope to the shoreline (Fig. 4a). Locations of these sensors are (77^{o}42.556’ N, 14^{o}41.846’ E and 77^{o}43.451’ N, 14^{o}39.397’ E) are shown by red dots in Fig. 5a. Sampling interval of both sensors was 1 s. The measurements revealed a phase delay of the tide near Van Mijen shore of about 30 min in comparison with the tide near Bellsund shore of Akseløya Island (Marchenko et al, 2011).

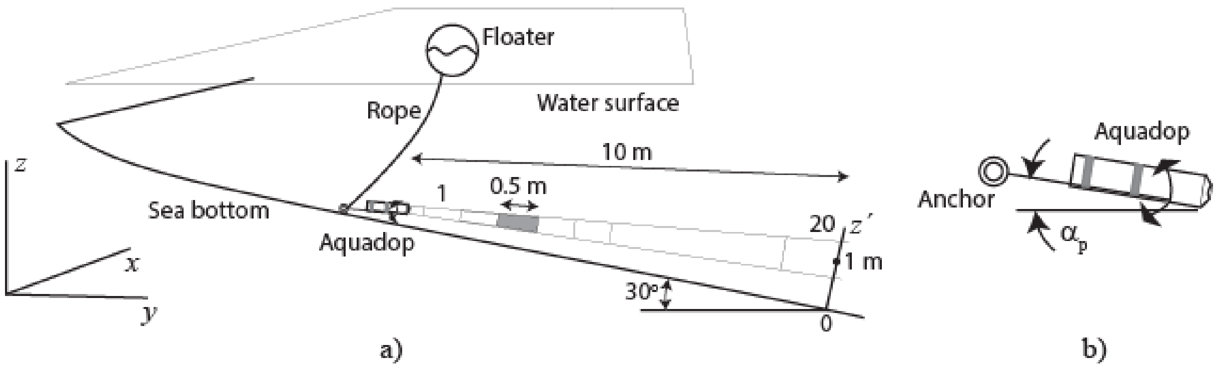

Figure 4. Deployment of ADCP Aquadopp (a) and its pitch angle α_p (b).

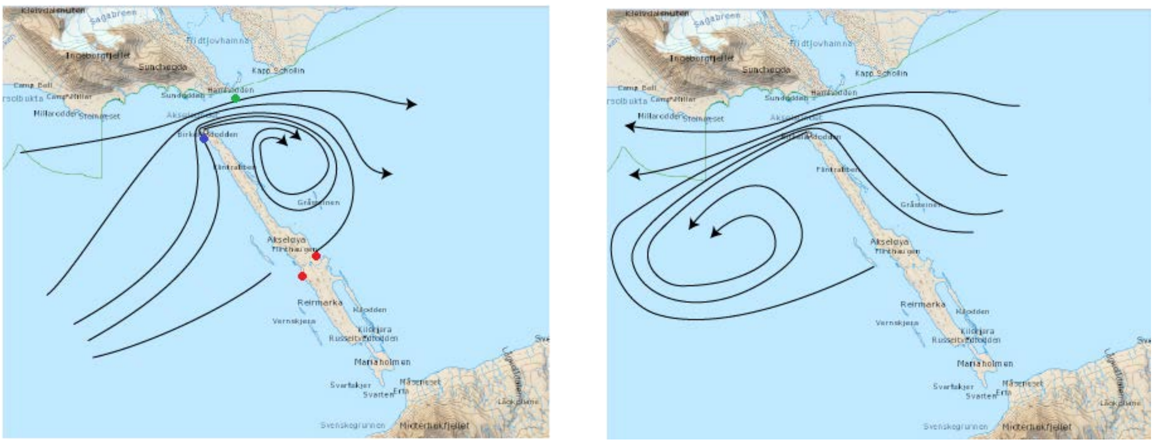

a) b)

Figure 5. Akseløya Island at the entrance to the Van Mijen Fjord. Qualitative scheme of flow lines in the Akselsundet Strait during the flood (a) and ebb (b) phases of the tide. Locations of field measurements are shown with red, blue, and green dots.

In August 2011 the SBE-37 CTD sensor (sampling frequency 6 s) was deployed near the northern tip of Akseløya Island from the side of the Bellsund Bay (blue dot in Fig. 5a). It was connected by a rope to a floating buoy. At the same time Acoustic Doppler Current Profiler equipped with a pressure sensor (Aquadopp, operating frequency 2 MHz) was deployed in the Akselsundet Strait (green dot in Fig. 5a with coordinates 77^o 45.367' N and 14^o 36.835' E) for the measurements of sea current velocity and water pressure (Fig. 4). The ADCP was mounted to a steel anchor and deployed at a bottom slope with pitch angle $\alpha_p \approx$-30^o at a depth of 20 m. The anchor was connected to a floating buoy by a rope (Fig. 4a). Small inclination of the ADCP axis to the bottom surface provided records of sea current velocities within a boundary layer of 1 m thick near the bottom (Fig. 4a). The ADCP recorded the data with a sampling interval of 60 s in 20 cells with a bin size of 0.5 m. The time variations of the water pressure measured at the points marked with blue and green dots in Fig. 5a are shown in Fig. 6a by blue and green lines. The time axis in Fig. 6a is local time on August 30 starting from 12:00. The records in Fig. 6a show the difference of tidal phases in the blue and green dots about 1h, i.e. flood and ebb tide are occurred at the green dot 1 h later than at the blue dot.

Figure 7a shows the absolute values of horizontal velocity measured by the ADCP at different distances from the sea bottom laid off along axis z shown in Fig. 4a. Figure 7b shows vertical velocities measured at the same locations. Nonzero vertical velocities near the bottom are explained by 30° bottom slope revealed by the pitch angle α_p of the ADCP (Fig. 4b). The maximal horizontal velocities exceed 1.5 m/s at 1 m distance from the bottom. The maximal horizontal velocities are below 0.5 m/s near the bottom. The maximal absolute vertical velocities are below 0.5 m/s near the bottom and reach 1 m/s at 1 m distance from the bottom. The heading angle of the ADCP changed its value during 2-3 hours from 100° to 240° during the high water tidal phase around t=15h and t=27h. The values of the pitch angle α_p changed during this time by 10°. Figure 8a shows a hodograph of horizontal velocities measured at different depths with the ADCP within 1 m boundary layer near the bottom. The maximal absolute values of velocities measured in the East-West directions reach 1 m/s, while the maximal absolute values of the South-North velocities are within 0.6 m/s.

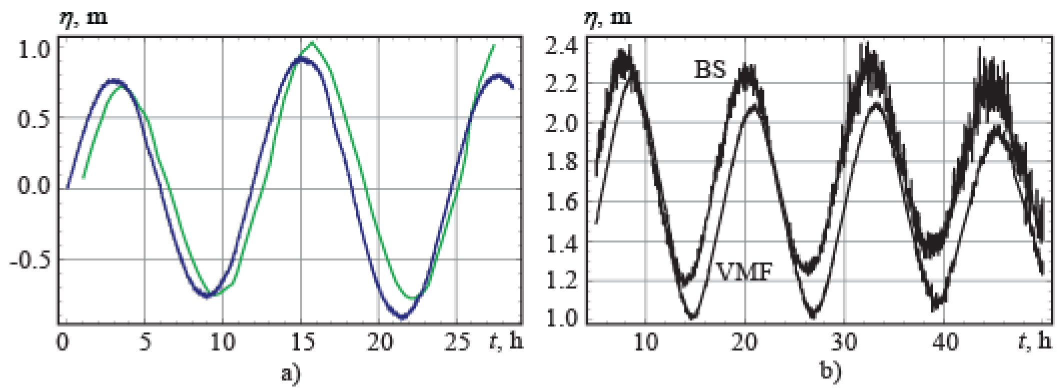

Figure 6. Water level elevations measured at the locations marked with blue and green dots (Fig. 5a) are shown with blue and green lines (a), and near Bellsund (BS line) and Van Mijen (VMF line) shores of Akseløya Island (b).

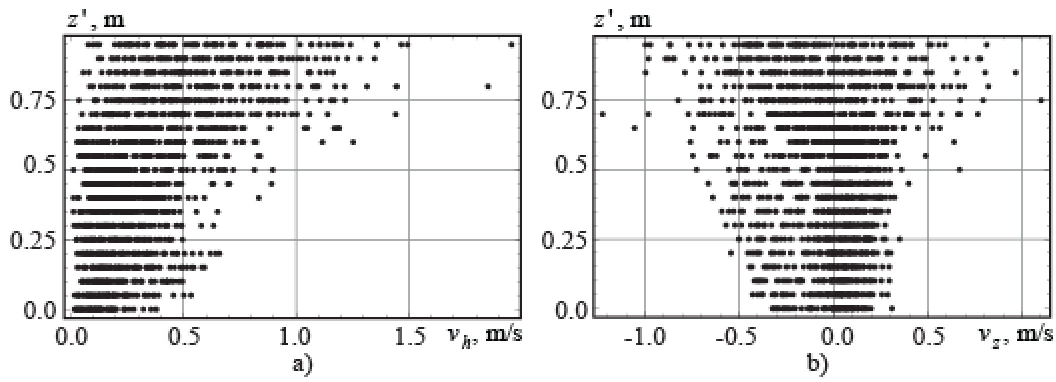

Figure 7. Vertical profiles of the horizontal (a) and vertical (b) velocities.

On September 24, 2013, two SBE-39 sensors were deployed with sampling interval 2 min at the locations shown by red dots in Fig. 5a and fixed on the shoreline by ropes. The sensors were taken out after one month. The sensors were pushed onshore due to wave action during storms in the beginning of October. Elevations of the water level recorded before the storm are shown in Fig. 6b. The time is accounted from 09:00 of September 24. Figure 6b shows that flood and ebb tides occurred on Van Mijen shore of Akseløya Island one hour later than on Bellsund shore of Akseløya Island.

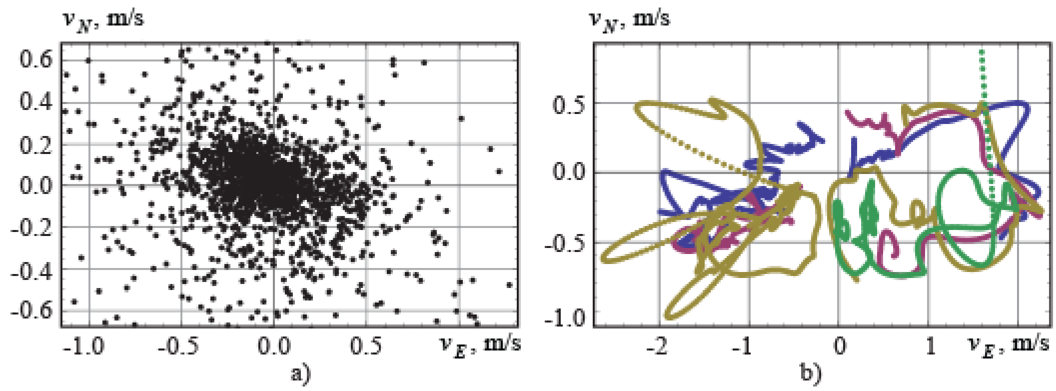

Figure 8. Hodographs of horizontal velocities in the Akselsundet Strait measured with ADCP (a) and surface drifters (b).

Trajectory of surface water particles and their velocities were investigated in September 2013 by the surface drifters equipped with GPS antennas AstroDog 320. Each drifter was constructed from 4 aluminum poles fixed on a vertical plastic pole. Submerged drogue was mounted on the aluminum poles. A weight was mounted at the bottom end of the vertical plastic pole and a buoyancy ring made from foam plastic was mounted at the top end of the plastic pole. Both kept the drifter in the vertical position. A GPS antenna was mounted on the top end of the plastic pole and its battery was protected by a plastic bag. The GPS signal from the antenna was recorded by the receiver with a sampling interval of 5 s. The operation range of the AstroDog system is 10 km on a flat area.

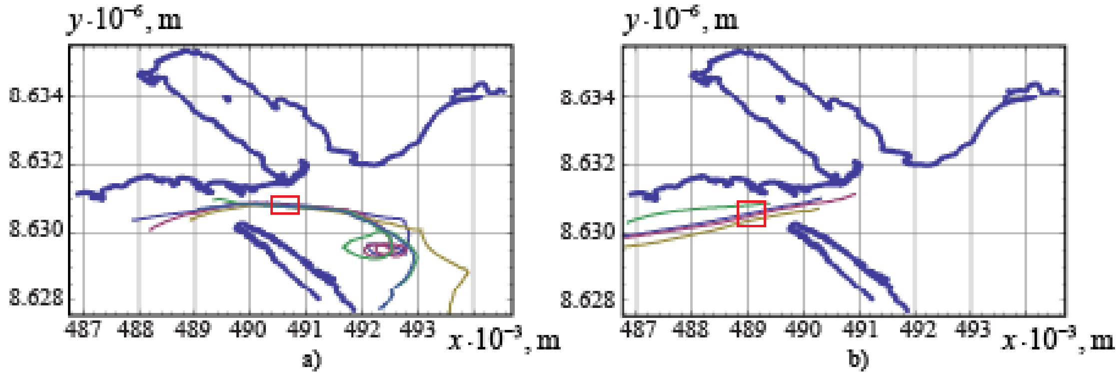

Figure 9.Trajectories of ice drifters deployed in the Akselsundet Strait during the flood (a) and ebb (b) tidal phases.

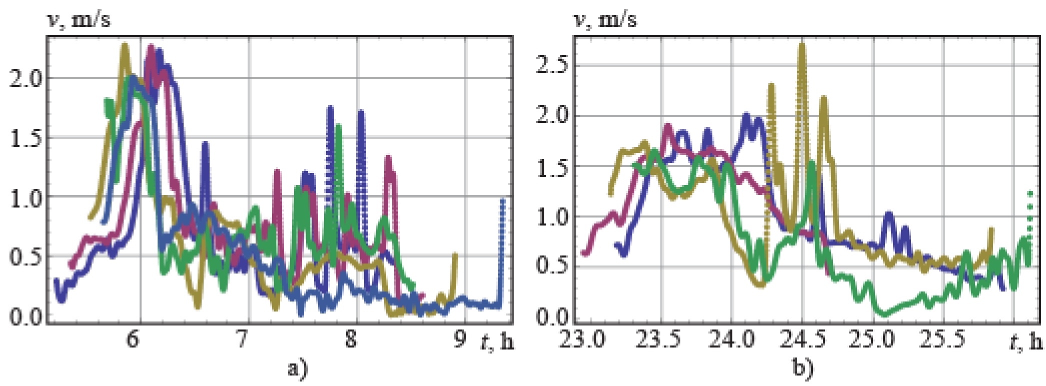

Figure 10. Absolute velocities measured by surface drifters during the flood (a) and ebb (b) tide.

Trajectories of the surface drifters recorded during the flood and ebb phases of the tide are shown in Fig. 9. Absolute velocities of the drifters are shown in Fig. 10 versus the time. The time in Fig. 9 corresponds to the time in Fig. 6b. During the flood phase the drifters deployed in different initial positions drifted through the Akselsundet Strait practically along the same trajectory showing the existence of a jet flow with strong current in the middle part of the strait. The water jet is located within the deepest area of the strait indicated by vertical rectangles S_0 and S_1 in Fig. 3b. The maximal speed of the drifters 2.5 m/s was measured during the flood phase of the tide around *t*=6h (Fig. 10a) when the drifters were inside the red square shown in Fig. 9a. During the ebb phase the maximal drift speed was recorded inside the red rectangle in Fig. 9b around *t*=24h (Fig. 10b). Other local maxima of the drift velocities in Fig. 10a are related to the rotation of the drifters captured by small eddies in the water jet. Figure 8b shows a hodograph of the drifters velocities measured when the drifters passed the Akselsundet Strait and their locations were between the red rectangles shown in Fig. 9a and Fig. 9b. It shows that the maximal speeds of the drifters in the east-west direction exceed 2 m/s. South velocity of drifters reached 1 m/s and North velocity of drifters was as high as 0.5 m/s.

AERIAL AND SATELLITE IMAGES

Satellite image provided by the Norwegian Polar Institute (Fig. 11a) shows the formation of eddies from the East side of Akseløya Island during the flood phase of the tide. Similar eddies are seen in Fig. 9a. An aerial image made by Trond Jensen at the ebb phase of the tide demonstrates the existence of a large eddy on the west side of the island (Fig. 11b). A qualitative scheme of the stream lines reconstructed by the analysis of trajectories of the surface drifters and satellite and aerial images is shown in Fig. 5a for flood phase of the tide and in Fig. 5b for he ebb phase of the tide. Sea current in the strait to the south of Akseløya Island is not taken into account in the scheme. The schemes in Fig. 5 show that a part of water around the Akseløya shore is not involved in the jet flow in the middle part of the Akselsundet Strait and participates only in the formations of eddies near the northern tip of the island. It is explained by the joint action of the sea bottom topography and friction between the water and seabed, the Coriolis force, and nonlinear hydrodynamics effects (the Coanda effect).

a) b)

Figure 11. Aerial images of the Akselsundet Strait when the water flow penetrates into the Van Mijen Fjord from Bellsund Bay (a) and when the current flows from the Van Mijen Fjord into Bellsund Bay (b).

NUMERICAL SIMULATIONS

High resolution tide model

A numerical model of the barotropic tides was used to investigate strong tidal currents and fine scale eddies observed in the vicinity of Akseløya Island. The computation domain in the western fjords of the Svalbard (see Fig. 1a) is based on the high spatial resolution with a grid size close to 90 m. The model is forced through the open boundary by five tidal constituents, namely: M2, S2, N2, K1, and O1. These data were adopted from the large scale computation made by Kowalik and Proshutinsky (1994). Figure 12 shows high resolution of the tidal currents in the Akselsundet Strait. The scheme in the left panel is related to the flood phase and in the right panel to the ebb phase. Strong currents are marked by the red and brown colours. The jet-like current of up to 250 cm/s is generated in the strait. The ebb and flood currents are directed by extremely variable different geometry of the fjord's shore and Akseløya Island.

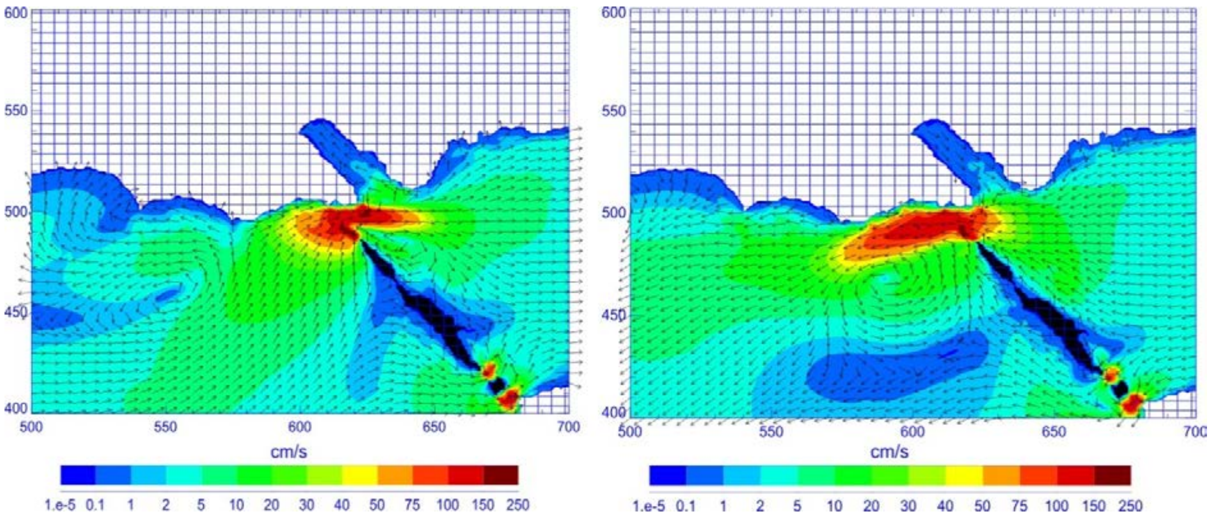

a) b)

Figure 12. Flood (a) and ebb (b) tidal currents computed using the numerical model by Kowalik and Proshutinsky (1994). Vectors define direction and colours correspond to the velocity magnitude in cm/s.

On the western side of the strait Akseløya Island orientation relative to the shore generated an obtuse angle, as the flood waters (Fig. 12b) are not strongly constrained by this geometry, therefore the flow through the strait does not entrain all the incoming waters. The part of the flow is deflected to the northern shore and backward to the west resulting in the large sluggish eddy. Concurrently at the eastern side of the passage the compact eddy is generated by the incoming flood flow (Fig 12a). The eddy's shape and strength is defined by the influence of Akseløya Island orientation relative to the shore. The ebb flow phase (Fig. 12b) on the eastern side of the passage due to acute angle between Akseløya and the fjord's shore shows the strong amplification of current. This jet-like current impinges on the water at the western side of the passage resulting in the large domain of the enhanced currents and the large eddy to south of the main flow. (The regular jet is associated with two eddies but the eddy at the northern side is damped by the shore). Fig. 12b actually shows two aspects of the jet-eddy interaction at Bellsund Bay, namely that on the one hand this large eddy is spawned by the jet but on the other hand the eddy is feeding the main jet as well. The influence of Akseløya

Island orientation relative to the shore is seen well when the areas of the enhanced current are compared with the flood/ebb patterns in Fig. 12.

Simplified box model of the tide

Simplified box model of the tide was developed for the description of tidal current and water level elevation in the strait connecting the Vallunden Lake and Svea Bay in the end of the Van Mijen Fjord (Marchenko and Morozov, 2013). In this approach equations of mass and momentum balance integrated over the strait volume are used to express the speeds of the jet flow at the ends of the strait by the water level elevations at the ends of the strait. Then the equation of mass balance in the Van Mijen fjord is used to calculate the elevation of water level in the fjord while the water level variation in Bellsund Bay is prescribed. Geometrical parameterization of seabed topography in the strait is used to derive the model equations. In this paper we consider the parameterization of the deepest part of the Akselsundet Strait where the jet flow is observed. The law of mass balance in the fjord is written in the form

$$S_{VM}\frac{d\eta_1}{dt} = S_1 u_1 , \tag{1}$$

where $\eta_1(t)$ is equal to the elevation of the water level in the Van Mijen fjord, S_1 is the area of vertical cross-section of the water jet penetrating in the fjord through the channel (Fig. 3b), and u_1 is the water speed averaged over the area S_1. The area of water surface S_{VM} in the Van Mijen Fjord is about 600 km^2.

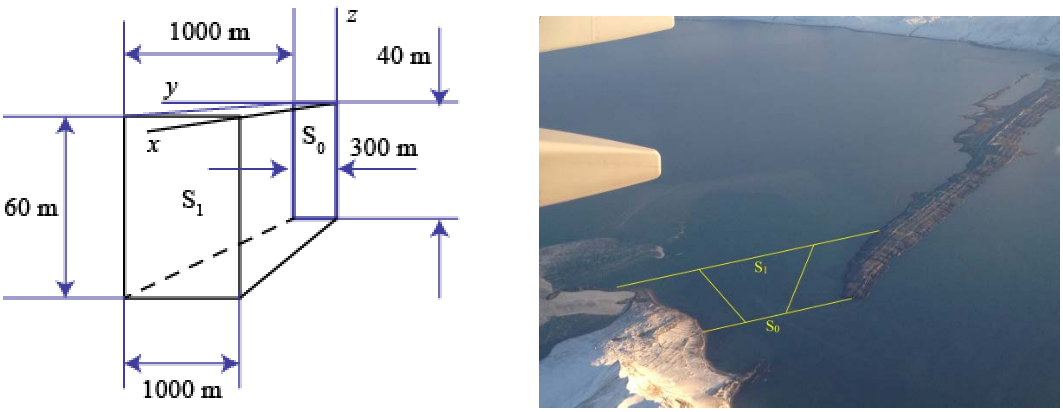

a) b)

Figure 12.Dimensions of the jet flow in the Akselsundet Strait (a). Location of the jet flow on the aerial photo (b).

Spatial configuration and dimensions of the channel with jet flow in the Akselsundet Strait are shown in Fig. 12. The length of the channel in the *x*- direction is L=1 km. The sea depth changes from h_0=40 m to h_1=60 m along the channel. The vertical cross-sections of the channel are rectangular. The width of the channel is equal to B_0=300 m at Bellsund boundary and B_1=1000 m at Van Mijen boundary of the channel. Figure 12b shows the location of the jet flow on the aerial photo made on October 10, 2013 at 13:50 of the local time.

Total water depth is denoted as H_0 at Bellsund and H_1 at Van Mijen boundaries of the channel, and undisturbed water depth is equal to h_0=H_0-η_0 at Bellsund and h_1=H_1-η_1 at Van Mijen boundaries of the channel. Water level variation at Bellsund boundary of the channel (forcing) is determined by function

$$\eta_0 = A_{M2}\cos(\omega_{M2}t - G_{M2}) + A_{S2}\cos(\omega_{S2}t - G_{S2}) + A_{K1}\cos(\omega_{K1}t - G_{K1}) + \\ + A_{N2}\cos(\omega_{N2}t - G_{N2}) + A_{O1}\cos(\omega_{O1}t - G_{O1}), \quad (2)$$

where numerical values of harmonic constants A, ω, and G are given in Table 2.

Table 2.Characteristics of tidal constituents.

	M2	N2	S2	K1	O1
A, m	0.485	0.113	0.184	0.06	0.024
ω, day^{-1}	0.0805114	0.07899925	0.08333334	0.04178075	0.03873065
G, rad	6.2	5.8	0.8	4.4	1.4

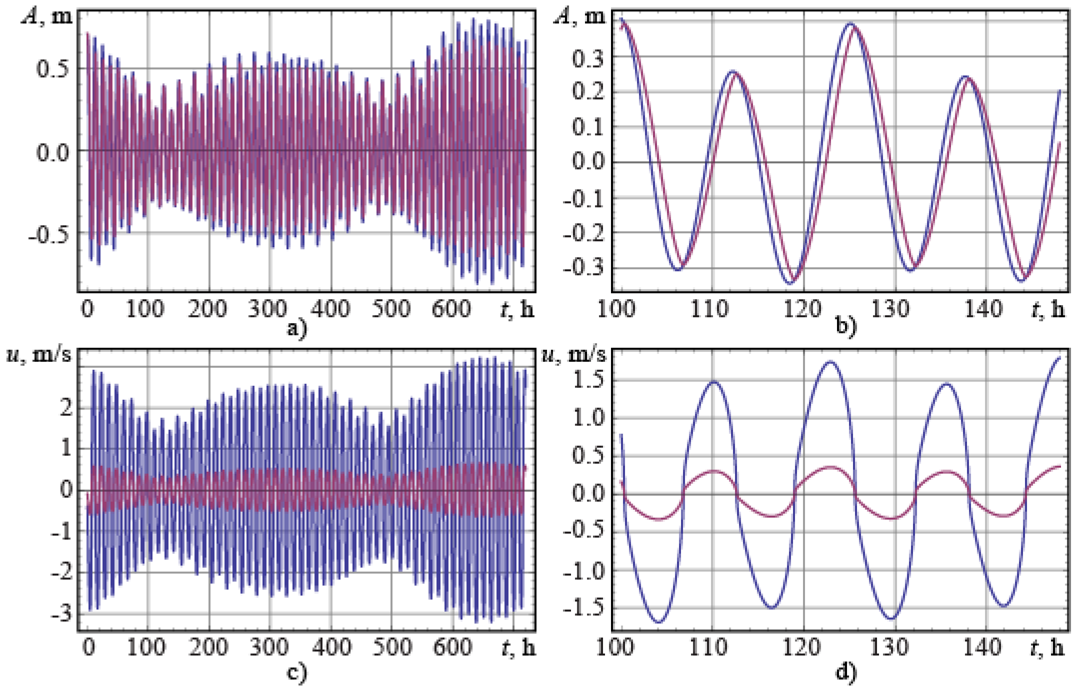

Figure 13. Model calculations of the water level (a,b) and sea current speed (c,d) during one month (a,c) and 48 hours (b,d). Blue and purple lines are related to Bellsund and Van Mijen baundaries of the channel with jet flow in the Akselsundet Strait.

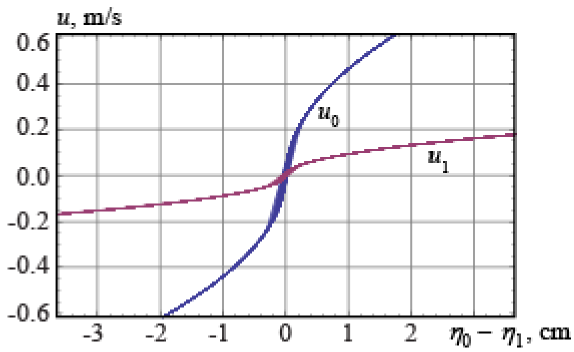

Figure 14. Water speeds at the boundaries of the channel versus the difference of the water levels at the boundaries of the channel.

The results of the numerical simulations during 30 days are illustrated in Fig. 13. Figure 13a shows that the variations of the water level at Bellsund (L) and Van Mijen (R) boundaries of the channel are similar, but tidal amplitude on Bellsund boundary of the channel is slightly higher. There is a phase shift about 0.5 h between tides at Bellsund and Van Mijen boundaries of the channel (Fig.13b). Figure 13c shows that the maximal speed of sea current at Bellsund boundary of the channel reaches 3 m/s during the maximal tide, while the maximal water velocities at Van Mijen boundary of the channel are close to 0.5 m/s. This effect is explained by the extension of the channel in the eastern direction (Fig. 12b). Figure 14 shows water speeds at the boundaries of the channel versus the difference of the water levels at the boundaries of the channel. It is seen that the water speed at Bellsund boundary of the channel is smaller 0.5 m/s when $|\eta_0 - \eta_1|<1$ cm. The navigable window is calculated using the following formula

$$T_N = \sum_{i=1}^{30\times24\times3600} \mathrm{UnitStep}[0.01\,\mathrm{m} - |\eta_0 - \eta_0|_{t=i}](2\cdot3600\cdot N)^{-1}, \quad (4)$$

where function UnitStep[z] is equal to 1 when $z>0$ and 0 when $z<0$, and $N=58$ is the amount of semidiurnal tide cycles in 30 days. Numerical estimates show that $T_N=13.66$ min.

CONCLUSIONS

Field investigations around Akseløya Island confirmed that the phase shift is about 0.5h -1h between the semidiurnal tide in the Van Mijen Fjord and Bellsund Bay. This phase shift creates water level gradient over the Akselsundet Strait and influences the generation of tidal currents with maximal speeds up to 3 m/s. The jet flow is formed inside the Akselsundet Strait within its deepest part approximately 300 m wide. Mean duration of the time window when the water speed in the strait is lower than 0.5 m/s is about 15 min, while the actual size of the window is varying from neap to spring tide.

The authors wish to acknowledge the support of the Research Council of Norway through the SFI project SAMCoT, SIU foundation through the project CPRU-2011/10042 SMIDA, logistic support provided by Lars Frode Stangeland and Odd Magne Kvalshagen (UNIS logistic), and Spitsbergen hunter Tommy Sandal.

REFERENCES

Kowalik, Z. and A. Yu. Proshutinsky, 1994. The Arctic Ocean tides, In: The Polar oceans and their role in shaping the global environment: Nansen Centennial Volume, Geoph. Monograph 85, AGU, 137-158.

Marchenko, A., Shestov, A., Karulin, A., Morozov, E., Karulina, M., Bogorodsky, P., Muzylev, S., Onishchenko, D., Makshtas, A., 2011. Field studies of sea water and ice properties in Svalbard fjords. POAC11-148, Montreal, Canada, 13 pp.

Marchenko, A.V., Morozov, E.G., 2013. Asymmetric tide in Lake Vallunden (Spitsbergen), Nonlinear Processes in Geophysics. 20, 935-944.

Stigebrandt A., 1980. Some aspects of tidal interactions with fjord constrictions, Estuarine and coastal marine science, Vol. 2, 151-166.

The Norwegian pilot. Sailing Directions. Svalbard and Van Mijen. The Norwegian Hydrographic Service and Norwegian Polar Institute, 2014.